Electronic Supporting Information

Approach for quality deep-ultraviolet nonlinear optical crystals via a substitution strategy of channel species in zeolite

Mingfeng Liu,[a] Yinggan Zhang,[a] Shuai-Hua Wang,[b] Shao-Fan Wu,[b] Jin-Xiao Mi,[a] Ya-Xi Huang [a,*]

[a]College of Materials, Xiamen University, Xiamen 361005, China

[b]Fujian Institute of Research on the Structure of Matter, Chinese Academy of Sciences, Fuzhou 350002, China

*Corresponding author Email: yaxihuang@xmu.edu.cn

1. Characterizations

1.1 X-ray Diffraction (XRD)

Powder XRD (PXRD) measurements were applied to check the purity of the resulting products which were performed on a Bruker D8 Advance powder X-ray diffractometer with Cu K_α radiation (λ = 1.5418 Å, 40 kV and 40 mA). The 2θ range was 5 - 60° with step size of 0.01° and fixed time of 0.1 s. Crystal data of single crystal X-ray Diffraction of **CLNSFZP** were collected on a Rigaku Oxford Diffraction with graphite monochromatic Mo Kα radiation (λ = 0.71073 Å, 45 kV/30 mA) at 100(2) K.

PXRD measurements of the pristine sample and the calcined samples at different temperature were performed on a Bruker D8 Advance powder X-ray diffractometer with the same condition. Owing to the calcined samples contaminated with alumina crucibles, an Al_2O_3 plate substrate was used to measure the PXRD pattern of pristine sample.

1.2 Scanning Electron Microscopy (SEM).

The crystal morphologies of **CLNSFZP** were performed by a field-emission scanning electron microscopy (FE-SEM) system (Model SU70).

1.3 Thermal Analysis

Thermal stabilities of **CLNSFZP** were analyzed by thermogravimetric / differential thermal analysis (TG-DTA) on Setsys Evolution 18 (SETARAM, France) in the temperature range of room temperature to 1000 °C at a heating rate of 10 $^{o}C\cdot min^{-1}$ under a N_2 gas flow of 20 $mL\cdot min^{-1}$.

1.4 Fourier Transform Infrared (FT-IR) Spectroscopy

FT-IR spectroscopy analysis was carried out on a Nicolet iS10 FT-IR spectrometer in the range of 400-4000 cm^{-1} in transmission mode at room temperature. A pellet made from pure powder samples mixed with KBr powder at the mass ratio of 1:100 has been used to record the spectra.

1.5 Ultraviolet-Visible-Near Infrared (UV-Vis-NIR) Diffuse Reflectance Spectroscopy

The UV-Vis-NIR diffuse reflectance spectra were recorded on a Varian Cary 5000 scan UV-Vis-NIR spectrometer in the spectral range of 200-800 nm at room temperature, by using $BaSO_4$ as the standard.

1.6 Theoretical Calculation

The first-principles calculations were performed within the Vienna ab initio simulation package (VASP)[1] based on the framework of density functional theory (DFT) using projector augmented wave (PAW) pseudopotentials within generalized gradient approximations of Perdew-Burke-Ernzerhof (GGA-PBE).[2, 3] The valence electron configurations are Cs($5s^25p^26s^1$), Zn($3d^{10}4s^2$), P($3s^23p^3$), O($2s^22p^4$), Na($2p^63s^1$), Li($1s^22s^1$), Si($3s^23p^2$),

F($2s^2 2p^5$),respectively. Then the crystal structures were relaxed through conjugate gradient algorithm with an energy convergence criterion of 1×10^{-4} eV. A plane-wave energy cutoff of 500 eV was chosen and the energy convergence criteria for electrons are increased to 1×10^{-6} eV for electronic self-consistent calculations. The automatically generated 3 × 3 × 7 *k*-point sampling was done using the Monkhorst-Pack scheme.

1.7 Second Harmonic Generation (SHG) Measurement.

The measurements of the powder second harmonic generation (SHG) effects were performed by using the modified Kurtz and Perry method at λ = 1064 nm generated by a Q-switched Nd:YAG solid-state laser.[4] An Andor DU420A-BR-DD CCD camera was used to measure the frequency-doubling signals of SHG. Single crystals were hand-picked from crystalline powder samples, then ground and sieved into several sets of different particle sizes. KDP (KH_2PO_4) with similar particle sizes was applied as the reference.

1.8 Single-crystal X-ray Diffraction

Suitable single crystals of **CLNSFZP** after examination under a polarized microscope have been selected for single-crystal X-ray diffraction. Crystal data were collected on a Rigaku Oxford diffractometer with graphite monochromatic Mo Kα radiation (λ =0.71073 Å, 45 kV/30 mA) at 100(2) K.

2. Synthesis

Single crystals of **CLNSFZP** have been synthesized via a modified fluoro-solvo-hydrothermal method by using triethylamine (TEA) as the solvent. The starting solid reactants (2 mmol $LiOH{\cdot}H_2O$, 1 mmol $ZnAc_2{\cdot}2H_2O$, and 1 mmol CsCl with a molar ratio of 2:1:1) were added into a 15 mL Teflon inline. Then, the excessive Na_2SiF_6 (9 mmol) solid powder was added to the reaction system acting as raw material and mineralizer. Then liquid media, TEA (2 mL, 14.9 mmol), deionized water (1.5 mL), and H_3PO_4 (85 wt%, 1.5 mL), were added sequentially without stirring. After that, the Teflon inline was sealed into the stainless-steel autoclave and put into an oven. After 72 hours of reaction at 230 °C, autoclaves were moved out from the oven and cooled down to room temperature in air. Finally, the solid product was washed with deionized water and dried in the air. Colorless rod-like crystals with an average diameter of 150-200 μm were obtained. The solid products were measured by powder X-ray diffraction (PXRD) to check their purity. After comparing the PXRD patterns of the products to the theoretical ones calculated from the single crystal XRD results, the high consistency reveals that the products are pure. These pure powder samples confirmed by PXRD were further used for other measurements as described below.

It is noted that Na_2SiF_6 plays a unique role in the formation of **CLNSFZP**. It acts not only as a raw material but also as a mineralizer. Based on the experimental results of our previously reported compound **CLNZP**, a highly concentrated NaF solution is essential in inhibiting the formation of the byproduct, $LiZnPO_4$,[5] which has the same color and shape as the product. Meanwhile, H_2O/OH^- groups are prevented from entering the reaction system under strong acidity and high fluoride concentration conditions, that is to form anhydrous compounds with

higher thermal stability. Therefore, to get **CLNSFZP**, excessive Na_2SiF_6 has been added into the reaction system of **CLNSFZP** as a substitute for NaF, which not only provides high fluoride concentration conditions but also changes the composition of the resulting compound to tune its thermal stability and other physical and chemical properties.

3. Volume calculation

The volume calculation of the 12-MR channel of a single unit cell for **CLNSFZP** and **CLNZP** was performed by following steps.

The 12-MR channel can be approximated as dodecagonal prism. The volume of dodecagonal prism can be obtained by

$$V = S_{us} \times h \qquad (1)$$

where S_{us} is the area of the upper surface of prism, and h is the height of prism.

The space occupancy rate of 12-MR channel was calculated by the volume of guest species resided in the 12-MR channel divided into the total volume of 12-MR channel of a unit cell.

Atomic radius used in the volume calculation[6]: O: 1.26 Å, Li: 0.76 Å, Na: 1.02 Å, Si: 0.54 Å, and F: 1.19 Å.

4. Crystal Structure Determination

The crystal structure was solved by direct methods and refined by the full-matrix least-squares technique using the SHELX programs,[7] included in the WinGX package,[8] and further checked for missing symmetry elements using PLATON.[9] The Li and Na atoms located at the channels are co-occupancy in the same position with the ratio of Li:Na ≈1 : 1. Meanwhile, Si has been defined as a half-occupancy because of the extremely large displacement parameter and in keeping the electric neutrality of the full crystal structure. The final refinement results convert to the formula as $\{(Li_3Na_3SiF_6)Cs_2\}[(ZnPO_4)_6]$. Crystallographic data and structural refinement results are listed in Tables S1−S4.

Table S1. Crystallographic data and structure refinement results for $\{(Li_3Na_3SiF_6)Cs_2\}[(ZnPO_4)_6]$ (**CLNSFZP**).

Chemical formula	$\{(Li_3Na_3SiF_6)Cs_2\}[(ZnPO_4)_6]$
Formula weight	1459.74
Crystal system	Hexagonal
Space group, Z	$P6_3$ (No. 173), 1
Temperature (K)	100(2)
a (Å)	12.4677(2)
c (Å)	4.98710(10)
V (Å^3)	671.35(3)
Radiation type	Mo Kα, λ = 0.71073 Å
μ (mm^{-1})	8.540
ρ (g·cm^{-3})	3.611
Crystal size (mm), color	0.50 × 0.30 × 0.15, colorless
T_{min}, T_{max}	0.0580, 0.2780
Reflections (independent, $I>2\sigma(I)$)	1077, 1017
No. of parameters	81
R_{int}, R_σ	0.0501, 0.0372
R_1, wR_2 ($I>2\sigma(I)$)[a]	0.0317, 0.0650
R_1, wR_2 (all)[a]	0.0349, 0.0667
GOF	1.099
Flack parameter	0.025(18)
$\Delta\rho_{max}$, $\Delta\rho_{min}$ (eÅ^{-3})	1.740, −0.696

[a] $R_1 = \sum \left| |F_O| - |F_C| \right| / \sum |F_O|$ and $wR_2 = \left[\sum w\left(F_O^2 - F_C^2\right)^2 / \sum w\left(F_O^2\right)^2 \right]^{1/2}$ for $F_O^2 > 2\sigma\left(F_O^2\right)$

Table S2. Fractional atomic coordinates and equivalent isotropic displacement parameters (Å^2) for $\{(Li_3Na_3SiF_6)Cs_2\}[(ZnPO_4)_6]$ (**CLNSFZP**).

Atoms	**Wyckoff Position**	***x***	***y***	***z***	U_{eq}	**Occupancy (<1)**
Cs1	2*b*	0.666667	0.333333	0.2901(2)	0.0112(2)	
Zn1	6*c*	0.34682(6)	0.41677(6)	0.3019(3)	0.0052(2)	
P1	6*c*	0.41060(14)	0.31892(14)	0.8032(8)	0.0043(4)	
O1	6*c*	0.5477(5)	0.4089(5)	0.7471(14)	0.0111(15)	
O2	6*c*	0.3850(6)	0.3034(6)	1.1040(12)	0.0101(12)	
O3	6*c*	0.3759(5)	0.1928(5)	0.6774(12)	0.0077(11)	
O4	6*c*	0.3287(5)	0.3653(5)	0.6775(12)	0.0083(12)	
Si1	2*a*	0.000000	0.000000	0.309(3)	0.0217(19)	0.5
Na1	6*c*	0.2522(8)	0.1239(6)	1.318(2)	0.035(3)	0.44(2)
Li1	6*c*	0.2522(8)	0.1239(6)	1.318(2)	0.035(3)	0.56(2)
F1	6*c*	0.9013(11)	0.0185(13)	0.072(3)	0.108(4)	

Table S3. Bond valence sums (BVS) calculations for $\{(Li_3Na_3SiF_6)Cs_2\}[(ZnPO_4)_6]$ (**CLNSFZP**).

Atoms	**Cs1**	**Zn1**	**P1**	**Li1 (×0.56)**	**Na1 (×0.44)**	**Si1(×0.5)**	**BVS**
O1	0.15/0.06 (0.15)(×3)/ (0.06)(×3)	0.56	1.27	-	-		**2.04**
O2	0.06 (0.06)(×3)	0.49	1.28	0.11 (0.11)	0.28 (0.28)		**2.01**
O3	-	0.53	1.23	0.13 (0.13)	0.31 (0.31)		**1.97**
O4	-	0.51	1.24	0.11 (0.11)	0.28 (0.28)		**1.93**
F1	-	-	-	0.09/0.19 (0.09)/(0.19)	0.22/0.45 (0.22)/(0.45)	0.55/0.43 (0.55)(×3)/ (0.43)(×3)	**0.94**
BVS	**0.81**	**2.09**	**5.02**	**0.63**	**1.54**	**2.94**	

+*n* is for the BVS of line atoms, (+*n*) is for the BVS of column atoms.

Table S4. Selected bond lengths and angles of $\{(Li_3Na_3SiF_6)Cs_2\}[(ZnPO_4)_6]$ (**CLNSFZP**).

Bond length	**Distance (Å)**	**Bond length**	**Distance (Å)**
Zn1–O1^{iii}	1.916(5)	Cs1–O1	3.111(6) (×3)
Zn1–O2^{ii}	1.968(6)	Cs1–O1^{ii}	3.438(7) (×3)
Zn1–O3^{iv}	1.943(6)	Cs1–O2^{ii}	3.468(6) (×3)
Zn1–O4	1.956(6)	Li/Na1–O2	2.277(10)
P1–O1	1.530(5)	Li/Na1^{ii}–O3	2.235(11)
P1–O2	1.526(8)	Li/Na1^{iv}–O4	2.281(9)
P1–O2	1.526(8)	Li/Na1–F1^{viii}	1.978(18)
P1–O4	1.536(6)	Li/Na1–F1^{ix}	2.240(18)
		Si1–F1^{i}	1.804(15) (×3)
		Si1–F1^{vi}	1.888(17) (×3)
Bond angle	**Angle (°)**	**Bond angle**	**Angle (°)**
O1^{iii}–Zn1–O3^{iv}	106.7(2)	O2–P1–O1	111.1(4)
O1^{iii}–Zn1–O4	114.2(3)	O2–P1–O4	108.2(4)
O3^{iv}–Zn1–O4	106.6(2)	O1–P1–O4	111.0(4)
O1^{iii}–Zn1–O2^{ii}	117.9(3)	O2–P1–O3	109.7(4)
O3^{iv}–Zn1–O2^{ii}	104.5(2)	O1–P1–O3	108.4(3)
O4–Zn1–O2^{ii}	105.9(2)	O4–P1–O3	108.5(4)
P1–O1–Zn1^{x}	133.4(4)	F1^{vi}–Si1–F1^{vii}	77.2(8) (×3)
P1–O2–Zn1^{xi}	120.8(3)	F1^{v}–Si1–F1^{i}	81.6(9) (×3)
P1–O3–Zn1^{xii}	128.6(4)	F1^{i}–Si1–F1^{vii}	100.6(3) (×3)
P1–O4–Zn1	121.7(4)	F1^{v}–Si1–F1^{vii}	177.1(10) (×3)

Symmetry codes: (i) $-x+y+1, -x+1, z$; (ii) $x, y, z-1$; (iii) $-x+1, -y+1, z-1/2$; (iv) $x-y, x, z-1/2$; (v) $x-1, y, z$; (vi) $y, -x+y+1, z+1/2$; (vii) $-x+1, -y, z+1/2$; (viii) $-x+y+1, -x+1, z+1$; (ix) $-x+1, -y, z+3/2$; (x) $-x+1, -y+1, z+1/2$; (xi) $x, y, z+1$; (xii) $y, -x+y, z+1/2$.

Table S5. The detailed volume calculation and space occupancy efficiency of the 12-MR channel of a single unit cell for $\{(Li_3Na_3SiF_6)Cs_2\}[(ZnPO_4)_6]$ (**CLNSFZP**) and $\{(Li_4Na_2O)Cs_2\}[(ZnPO_4)_6]$ (**CLNZP**).

	12-MR channel			
	Area of the upper surface (Å^2)	**Height (Å)**	**Volume (Å^3)**	**Space occupancy efficiency (%)**
CLNSFZP	27.55	2.57	70.72	89.57%
CLNZP	27.38	2.56	70.10	39.78%

Table S6. The dipole moment of individual [PO_4] group and [ZnO_4] group in the crystal structure of {($Li_3Na_3SiF_6$)Cs_2}[($ZnPO_4$)$_6$] (**CLNSFZP**).

PO_4 Dipole Moment Calculation Template

			Cartesian Coordinates			Distance (Å)	Unit Vector				Center of Gravity	Center of Charge	Dipole Moment for Each P-O Bond (debye)
Z	Atom	Charges	*x*	*y*	*z*		*x*	*y*	*z*	Unitized Vector			
15	P1	5.0187	0	0	0	0							
8	O2	-1.2814	0.16758	-0.22243	-1.49962	1.52526	0.10987	-0.14583	-0.98319	1	0.347826	0.4818314	18.89841
8	O1	-1.2647	-0.97154	1.1484	0.28028	1.53012	-0.63494	0.75053	0.18318	1	0.347826	0.4813813	18.87853
8	O4	-1.2428	-0.50078	-1.31023	0.62738	1.53658	-0.32591	-0.85269	0.40830	1	0.347826	0.4807907	18.85294
8	O3	-1.2298	1.36176	0.35358	0.62738	1.54046	0.88400	0.22953	0.40727	1	0.347826	0.4804404	18.83803

Parameter	-0.05904	Cell Volume	671.354	Å^3	Dipole Moment of PO_4				
		Z	1		*x*	*y*	*z*	Magnitude	
		Total Dipole Moment	0.001088042	debye/Å^3	0.598020101	-0.338969617	0.247073348	0.73046128	debye
			1.08804E-21	esu·cm/Å^3				7.30461E-19	esu·cm

ZnO_4 Dipole Moment Calculation Template

			Cartesian Coordinates			Distance (Å)	Unit Vector				Center of Gravity	Center of Charge	Dipole Moment for Each Zn-O Bond (debye)
Z	Atom	Charges	*x*	*y*	*z*		*x*	*y*	*z*	Unitized Vector			
30	Zn2	2.0863	0	0	0	0							
8	O4	-0.5065	0.36009	-0.43382	-1.87265	1.95568	0.184125	-0.221826	-0.95754418	1	0.210526	0.2335659	7.87691
8	O1	-0.5642	-0.7434	1.74429	0.2738	1.91577	-0.38804	0.91049	0.142919035	1	0.210526	0.2347780	8.13498
8	O3	-0.5255	-1.32646	-1.27539	0.6209	1.94206	-0.68302	-0.65672	0.319712058	1	0.210526	0.2339654	7.96182
8	O4	-0.4901	1.63633	-0.46873	0.98745	1.96783	0.83154	-0.238196	0.501796395	1	0.210526	0.2332214	7.80383

Parameter	-0.35194	Cell Volume	671.354	Å^3	Dipole Moment of ZnO_4				
		Z	1		*x*	*y*	*z*	Magnitude	
		Total Dipole Moment	0.002343451	debye/Å^3	-0.6552402	-1.428016901	0.081579518	1.573285479	debye
			2.34345E-21	esu·cm/Å^3				1.57329E-18	esu·cm

Table S7. The dipole moment of the total anionic framework of {($Li_3Na_3SiF_6$)Cs_2}[($ZnPO_4$)$_6$] (**CLNSFZP**).

	x	***y***	***z***	**All (Debye)**
CLNSFZP	0.000493	-1E-14	1.97192	**1.97192**

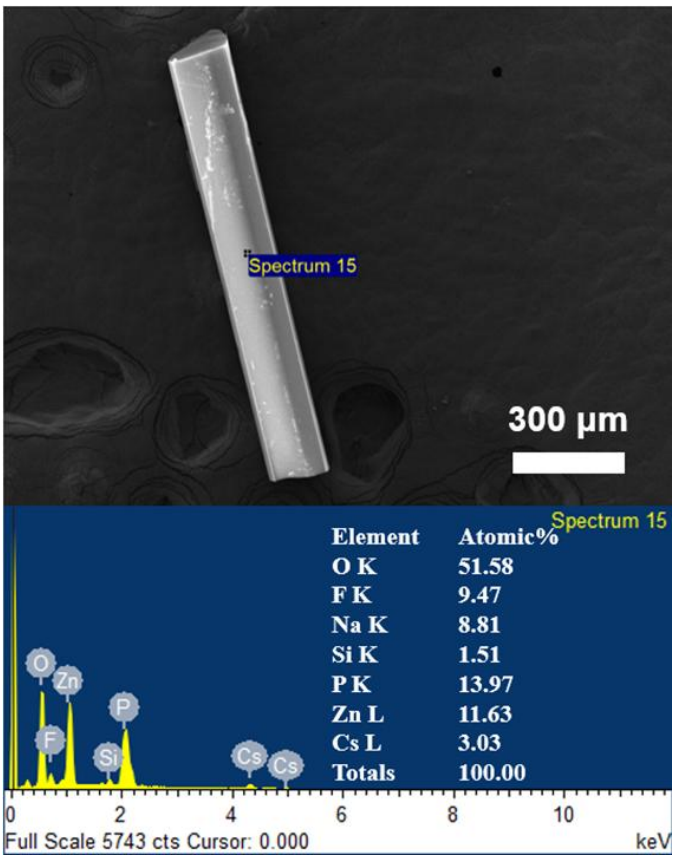

Figure S1. SEM and EDX results of a single crystal of $\{(Li_3Na_3SiF_6)Cs_2\}[(ZnPO_4)_6]$ (**CLNSFZP**).

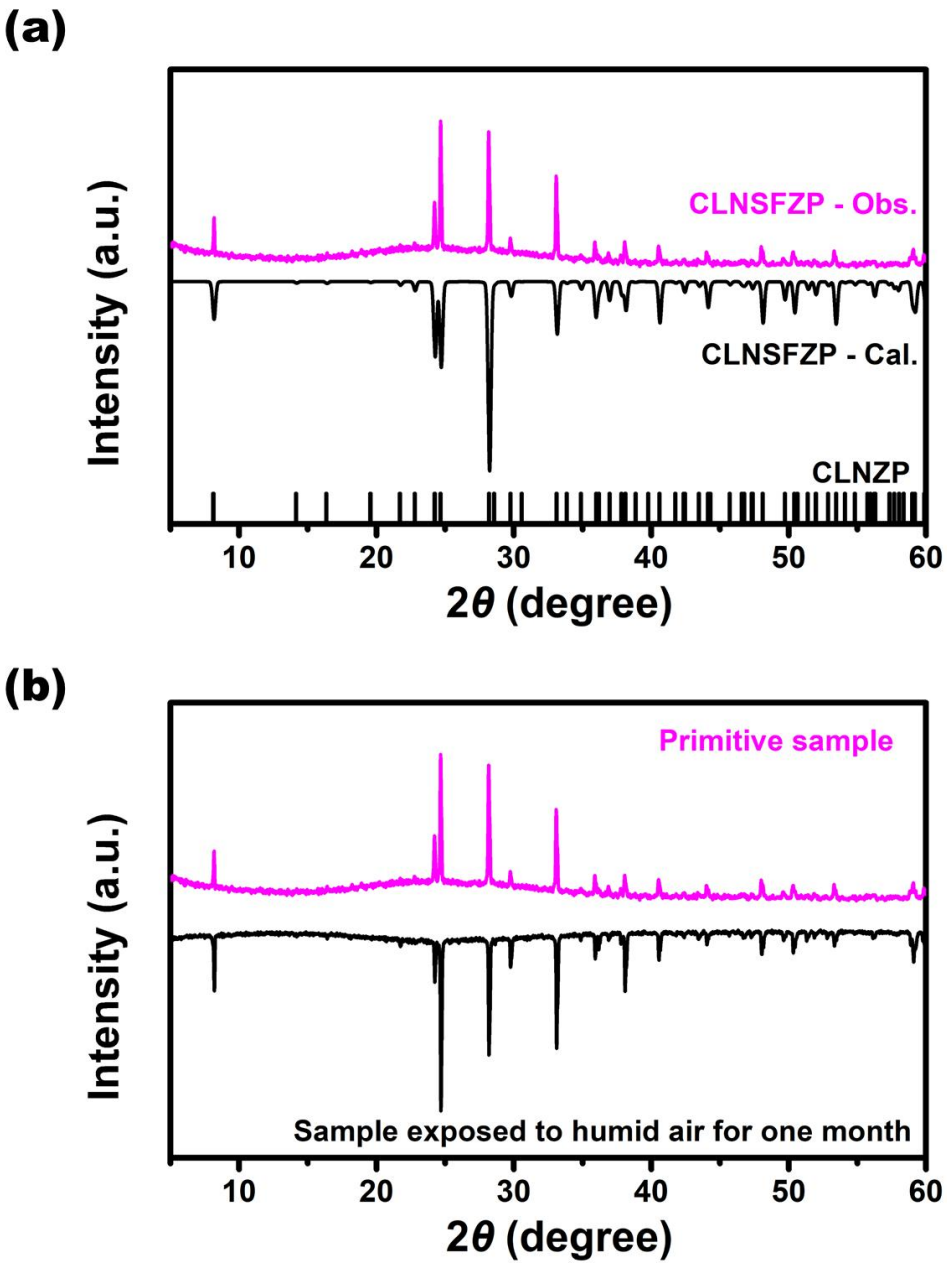

Figure S2. (a) PXRD patterns of $\{(Li_3Na_3SiF_6)Cs_2\}[(ZnPO_4)_6]$ (**CLNSFZP**) (pink pattern: experimental, black pattern: calculated, the black bar pattern at the bottom: calculated pattern of Bragg reflection positions of $\{(Li_4Na_2O)Cs_2\}[(ZnPO_4)_6]$ (**CLNZP**).[10] (b) The comparison between PXRD patterns of the primitive sample and sample exposed to humid air for one month.

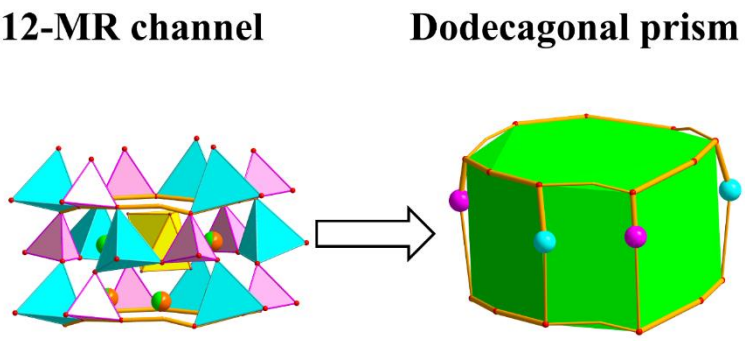

Figure S3. The sketch map of the 12-MR channel for $\{(Li_3Na_3SiF_6)Cs_2\}[(ZnPO_4)_6]$ (**CLNSFZP**).

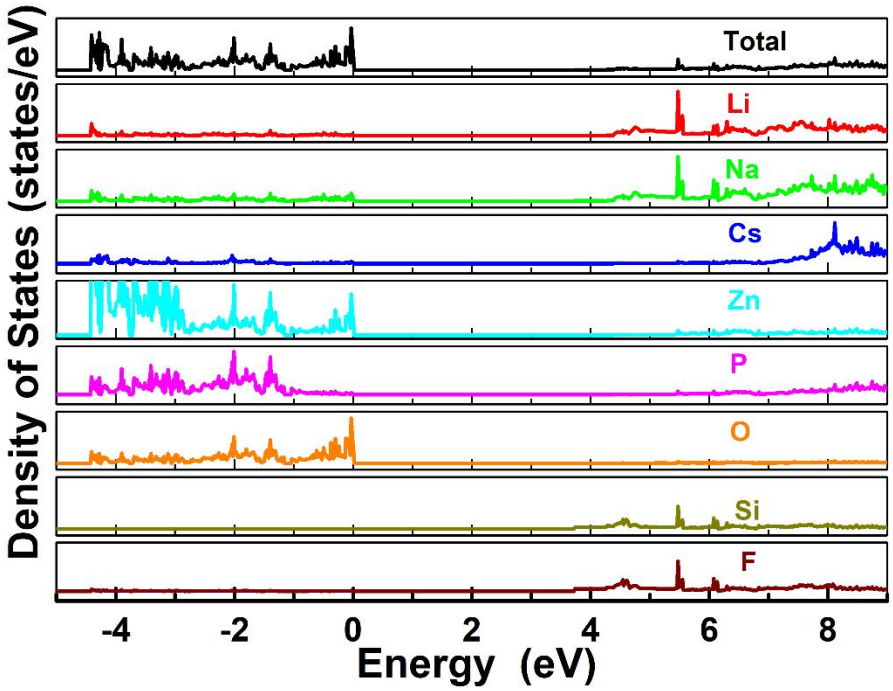

Figure S4. Total densities of states (TDOS) and partial densities of states (PDOS) for $\{(Li_3Na_3SiF_6)Cs_2\}[(ZnPO_4)_6]$ (**CLNSFZP**) from first-principles calculations.

References

1. J. Hafner, *Journal of Computational Chemistry*, 2008, **29**, 2044-2078.
2. J. P. Perdew, K. Burke and Y. Wang, *Physical Review B*, 1996, **54**, 16533-16539.
3. J. P. Perdew, K. Burke and M. Ernzerhof, *Physical Review Letters*, 1996, **77**, 3865-3868.
4. S. K. Kurtz and T. T. Perry, *Journal of Applied Physics*, 1968, **39**, 3798-3813.
5. H.-J. Wang, Z.-W. Jiao, T.-Q. Sun, R. Liang, S. Chen, Y. Cui and Y. Yang, *Chinese Journal of Structural Chemistry*, 2018, **37**, 603-610.
6. R. D. Shannon, *Acta crystallographica section A: crystal physics, diffraction, theoretical and general crystallography*, 1976, **32**, 751-767.
7. George and M. Sheldrick, *Acta Crystallographica Section C*, 2015, **C71**, 3-8.
8. L. Farrugia, *Journal of Applied Crystallography*, 1999, **32**, 837-838.
9. A. L. Spek, *Acta Crystallographica*, 2015, **71**, 9-18.
10. M. Liu, X.-Y. Tang, Y. Zhang, J. Ren, S. Wang, S.-F. Wu, J.-X. Mi and Y.-X. Huang, *Inorganic Chemistry*, 2023, **62**, 15527-15536.